C. R. Mecanique 340 (2012) 859–866

Contents lists available at SciVerse ScienceDirect

Comptes Rendus Mecanique

www.sciencedirect.com

Out of Equilibrium Dynamics

On the scaling of the mean length of streamline segments in various turbulent flows

Philip Schäfer, Markus Gampert, Norbert Peters *

Institute of Combustion Technology, RWTH Aachen University, Templergraben, 64, 52056 Aachen, Germany

ARTICLE INFO

Article history:
Available online 15 November 2012

Keywords:
Turbulence
Streamline segment
Scaling

ABSTRACT

The geometrical properties of streamline segments (Wang, 2010 [1]) and their bounding surface (Schaefer et al., 2012 [2]) in direct numerical simulations (DNS) of different types of turbulent flows at different Reynolds numbers are reviewed. Particular attention is paid to the geometrical relation of the bounding surface and local and global extrema of the instantaneous turbulent kinetic energy field. Also a previously derived model equation for the normalized probability density of the length of streamline segments is reviewed and compared with the new data. It is highlighted that the model is Reynolds number independent when normalized with the mean length of streamline segments yielding that the mean length l_m plays a paramount role as the only relevant length scale in the pdf. Based on a local expansion of the field of the absolute value of the velocity u along the streamline coordinate a scaling of the mean size of extrema of u is derived which is then shown to scale with the mean length of streamline segments. It turns out that l_m scales with the geometrical mean of the Kolmogorov scale η and the Taylor microscale λ so that $l_m \propto (\eta\lambda)^{1/2}$. The new scaling is confirmed based on the DNS cases over a range of Taylor based Reynolds numbers of $Re_\lambda = 50$–300.

1. Introduction

In the course of turbulence research a manifold of different strategies has been devised to explain the complex motion of a turbulent fluid flow. The spectrum of approaches reaches from purely mathematical theories based solely on the Navier–Stokes equations, such as two-point correlations which have yielded the famous and celebrated 4/5th law [3], to dimensional arguments which has led to the prediction of the $-5/3$rd scaling of the energy spectrum in the inertial subrange [4]. Another approach which has greatly benefited from the recent advances in high performance computing is to analyze turbulent inherent geometries. In 1971, Corrsin [5] asked the question: "What types (of geometry) are naturally identifiable in turbulent flows?". In this spirit, vortex structures have been identified and analyzed for instance by She et al. [6] and Kaneda and Ishihara [7]. They were found to form tubes in regions of high vorticity, while a sheet-like structure was identified in regions of low vorticity. However, vortex tubes and sheets do not allow a unique and space-filling decomposition of the flow field into unambiguous sub-ensembles. This problem was overcome by Wang and Peters [8,9] in their concept of dissipation elements, an approach which has its roots in early works by Gibson [10] who analyzed the role of extreme points in turbulent scalar mixing processes. This concept, based on gradient trajectories, allows the decomposition of turbulent scalar fields into smaller sub-units. By calculating gradient trajectories in direction of ascending and descending scalar gradients, a local minimum and a local maximum points are reached. Dissipation elements are then defined as

* Corresponding author.
E-mail addresses: pschaefer@itv.rwth-aachen.de (P. Schäfer), mgampert@itv.rwth-aachen.de (M. Gampert), n.peters@itv.rwth-aachen.de (N. Peters).

1631-0721/$ – see front matter
http://dx.doi.org/10.1016/j.crme.2012.10.032

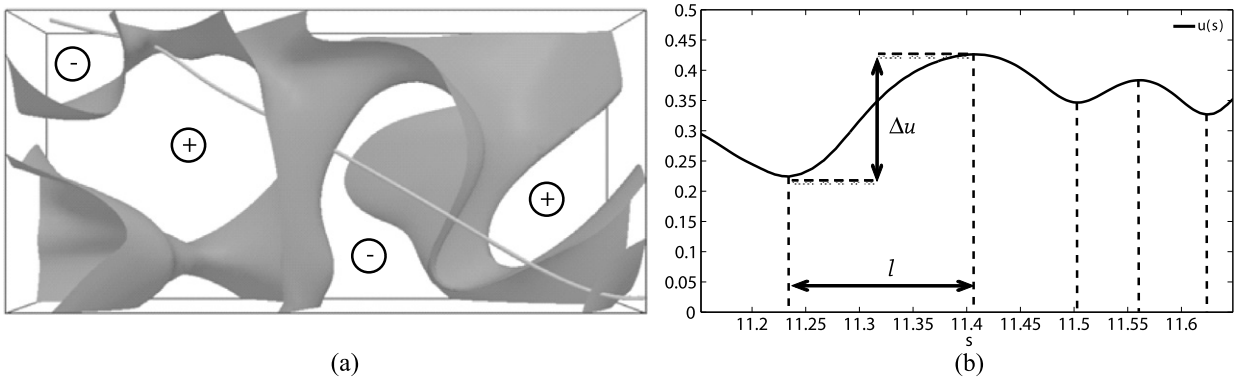

Fig. 1. (a) Isosurface defined by $u_s = 0$ and streamline. (b) Variation of u along the streamline over the arclength s and parametrization of a positive segment with its length l and velocity difference Δu.

the spatial region from which all gradient trajectories reach the same pair of maximum and minimum points in a scalar field. They may then be parameterized by the linear distance between and the scalar difference at the extreme points which makes them amenable to statistical analysis. The most important feature of dissipation elements is that they are space-filling and unambiguous, meaning that at any instant in time the turbulent scalar field can be decomposed in a determined manner. Then, based on the much simpler conditional statistics within the dissipation elements and the knowledge of their statistical distribution (in terms of joint probability density functions) the complicated statistics of the entire scalar field can be reconstructed. Successful examples of this approach can be found in [11,1]. However, one major shortcoming of the theory of dissipation elements is that it is only applicable to turbulent scalar fields. In order to also apply this successful theory to the turbulent velocity field itself, Wang [1] proposed to study streamlines in turbulent velocity fields. The geometrical properties of particle paths (the analogon to streamlines in an evolving turbulent field) have for instance been studied by Rao [12], Braun et al. [13] and Scagliarini [14], whose ideas have been extended to the geometrical properties of streamlines by Schaefer et al. [15]. Streamlines are not Galilei invariant, meaning that the chosen frame of reference determines the streamline topology. Thus, one has to choose an appropriate frame of reference when analyzing turbulent flow fields based on streamlines. In the course of this work this frame of reference will be the fluctuating velocity field with zero mean for two reasons: first, from a geometrical point of view we are only interested in the geometry and topology of the fluctuating field, which is often used to isolate "pure" turbulent physics without the interaction with solid walls, mean gradients or alike. Second, it has been shown that there exists a frame, in which the so-called streamline persistence is maximized [16]. Streamlines are considered persistent if their geometry changes slowly enough for a particle to approximately follow their path for a significantly long time. In that case, particles initially close to each other will only separate once they approach a straining stagnation point, where streamlines diverge. For isotropic turbulence, three of the cases considered in this work, it could be shown that the appropriate frame of reference is the one where all mean velocity components vanish, i.e. the fluctuating velocity field [17]. In Section 2 we will review the most important features of streamline segments and the bounding surface of the latter in space. In Section 3 the four different DNS cases which are the basis of the present work will be introduced. In Section 4 the model for the length distribution of streamline segments and the physical reasoning behind the different terms in the model equation will be discussed. In Section 5 a new scaling for the mean length of streamline segments is derived and compared with the DNS data. Finally, in Section 6 concluding remarks are given.

2. Streamline segments and related geometries

Integration of

$$\mathrm{d}x_i = u_i\big(x_j(\hat{t}), t_0\big)\,\mathrm{d}\hat{t} \tag{1}$$

where $u_i(x_j(\hat{t}), t_0)$ denotes the i-th velocity component of a turbulent velocity field at position x_j and time t_0 and a pseudo-integration time $\hat{t}$, yields a space curve $\Gamma(\hat{t})$ which is known as a streamline. However, different from gradient trajectories (based on any turbulent scalar field) which inevitably end in a local extreme point (where the gradient of the scalar vanishes) [8,9], streamlines are a priori infinitely long. This is why Wang [1] proposed to partition them into segments based on local extrema of u along the streamline, i.e. points where the gradient of u in streamline direction $u_s \equiv t_i \partial u/\partial x_i = \partial u/\partial s$ vanishes. It turns out that when u_s is treated as a scalar field all streamline segment ending points lie in an isosurface defined by $u_s = 0$, which divides space into two regions, one of which contains all positive segments where $u_s > 0$ while the other one contains all negative segments where $u_s < 0$. Fig. 1(a) shows this isosurface as well as a streamline entering the box at the top left corner and leaving it at the bottom right corner. In between, the streamline intersects the isosurface five times, thus yielding four streamline segments. Fig. 1(b) shows the variation of u along the streamline as well as the four streamline segments.

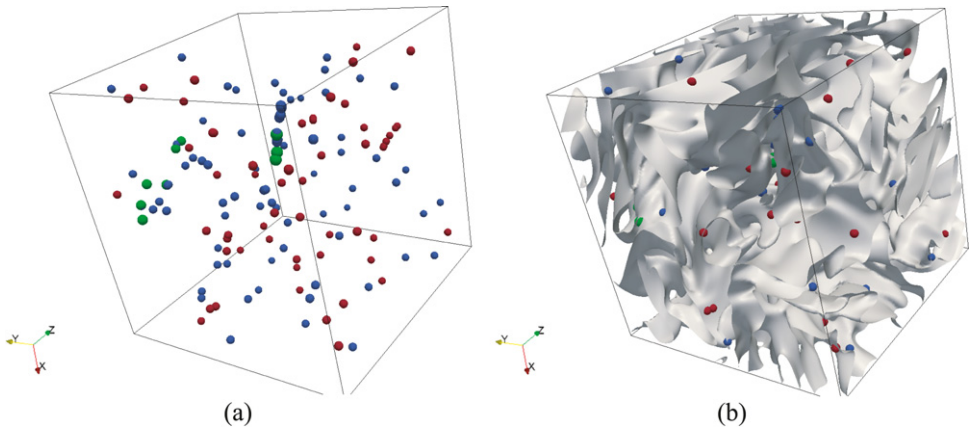

Fig. 2. (a) Local extreme points (blue: minima, red: maxima, green: stagnation points) of the turbulent kinetic energy field (taken from DNS). (b) Local extreme points and the surface $u_s = 0$.

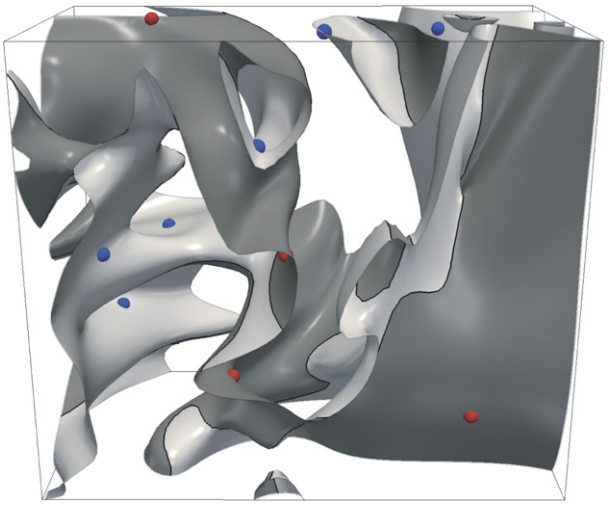

Fig. 3. Minimal (light gray) and maximal (dark gray) parts of the isosurface $u_s = 0$.

Apart from the extrema of the absolute value of u in streamline direction, the isosurface $u_s = 0$ also contains all local extrema of the instantaneous turbulent kinetic energy field $k = u/2$ as all points where the gradient $u\nabla u = \nabla k \equiv 0$ must lie in the surface [2]. These points also include all stagnation points of the turbulent velocity field, which are critical points where all three velocity components $u_i = 0$. As at these points $k = 0$, they are absolute minimum points of the kinetic energy field [15]. A local expansion of the isosurface in the vicinity of a stagnation point has revealed that indifferent of the type of stagnation point (in general there exist four different types of stagnation points in incompressible flows [18]) the surface is always a quadric of cone type which means that at the stagnation point two folds of the surface come infinitely close to each other [15].

Fig. 2(a) shows the distribution of local extrema (i.e. points where $\nabla k = 0$) obtained from the DNS of homogeneous isotropic turbulence in a 2π-periodic box, while Fig. 2(b) shows their geometrical relation with the isosurface and proofs that they are all located in the isosurface. In addition, Schaefer et al. [2] have shown that the surface can be further decomposed into two parts, one containing all maximum points and one containing all minimum points. The demarcation line on the surface is the ensemble of points where the streamline is perpendicular to the surface. This is shown in Fig. 3 where the light gray area is the minimal part of the surface while the dark gray area is the maximal part.

3. DNS

The following quantitative statistical analysis of turbulent flows by means of streamline segments is based on four different DNS calculations in a 2π-periodic box. These comprise three homogeneous isotropic turbulent fields, two of which are decaying while the third one is forced such that the turbulence intensity is statistically stationary. The fourth case is that of homogeneous shear turbulence with a mean shear gradient. These DNS cases allow for an analysis of the influence of the Reynolds number as well as that of the flow type on the statistics of streamline segments. For brevity, details apart

Table 1
Parameters of the different DNS cases.

DNS case	1	2	3	4
Flow type	Decaying	Decaying	Forced	Shear
No. of grid cells	1024^3	1024^3	1024^3	1024^3
Reynolds number Re_λ	50	116	206	300
Viscosity ν	5×10^{-4}	1×10^{-4}	2.0×10^{-3}	5×10^{-4}
Kinetic energy k	4.9×10^{-2}	3.4×10^{-2}	12.0	3.07
Dissipation ε	1.3×10^{-2}	5.9×10^{-3}	11.3	1.39
Kolmogorov scale η	0.01	3.6×10^{-3}	5.2×10^{-3}	3.1×10^{-3}
Taylor length λ	0.139	7.6×10^{-2}	0.146	0.105
Integral time τ_{int}	3.88	5.76	1.06	2.21
Kolmogorov time τ_η	0.196	0.130	0.013	0.019
Resolution $\Delta x/\eta$	0.610	1.69	1.19	1.98
Mean shear S	–	–	–	1.5

from Table 1 which summarizes the most important statistical quantities of the flow fields, are not given. The reader is referred to [19,20] which contain detailed descriptions of the cases under consideration as well as the numerical procedures employed.

4. A model for the length distribution of streamline segments

To go beyond a mere descriptive stage of turbulent flows by means of streamlines and related geometries Wang [1] proposed to parametrize streamline segments using the arclength distance l between and the velocity difference Δu at the ending points. Then most of the statistical information are captured in the joint probability density function (jpdf) of these two parameters $P(l, \Delta u)$. Based on Bayes' theorem we relate the marginal distribution of the length of streamline segments $P(l)$ to the conditional pdf $P(\Delta u|l)$ yielding

$$P(l) = \frac{P(l, \Delta u)}{P(\Delta u|l)} \tag{2}$$

Based on prior works, Schaefer et al. [2] derived a model equation for the normalized probability density function of the length of streamline segments $\tilde{P}(\tilde{l}) = P(l/l_m) \cdot l_m$ (Eq. (3)), where l_m denotes the mean length of streamline segments whose scaling with turbulent length scales is discussed in Section 5.

$$\begin{aligned}\frac{\partial \tilde{P}(\tilde{l}, \hat{\tau})}{\partial \hat{\tau}} + \frac{\partial}{\partial \tilde{l}}\left[\left(\tilde{a}_1(\tilde{l}) - \frac{\tilde{l}}{\tau_{lm} a_\infty}\right)\tilde{P}(\tilde{l}, \hat{\tau})\right] &= \frac{1}{2}\frac{\partial^2}{\partial \tilde{l}^2}\left[\tilde{a}_2(\tilde{l})\tilde{P}(\tilde{l}, \hat{\tau})\right] \\ &\quad + \Lambda_c\left(2\int_0^\infty \tilde{P}(\tilde{l} + \tilde{z}, \hat{\tau})\,\mathrm{d}\tilde{z} - \tilde{l}\tilde{P}(\tilde{l}, \hat{\tau})\right) \\ &\quad + 2\Lambda_a\left(\int_0^{\tilde{l}} \frac{\tilde{y}}{\tilde{l}}\tilde{P}(\tilde{l} - \tilde{y}, \hat{\tau})\tilde{P}(\tilde{y}, \hat{\tau})\,\mathrm{d}\tilde{y} - \tilde{P}(\tilde{l}, \hat{\tau})\right)\end{aligned} \tag{3}$$

For a detailed derivation of Eq. (3) the reader is referred to [2]. In the following the different terms will briefly be discussed and related to their physical sources. The different terms in Eq. (3) represent the different mechanisms which influence the temporal length evolution of streamline segments belonging to a length class l. The first term on the l.h.s. is the unsteady term which in the numerical solution is sought to vanish to obtain a steady solution. The second term on the l.h.s. and the first term on the r.h.s. describe so-called "slow changes" of streamline segments, where $\tilde{a}_1$ denotes the normalized drift velocity in phase space and $\tilde{a}_2$ denotes the normalized diffusion in phase space. Physically, the drift $\tilde{a}_1 = \tilde{v}_D + \widetilde{\langle \Delta u|l \rangle}$ can be decomposed into two different parts, one is the diffusive drift of small segments which turns out to scale as $\tilde{v}_D \propto -1/\tilde{l}$ yields the disappearance of small segments due to viscous diffusion. The second one is due to the conditional velocity difference at the ending points of streamline segments which yields a continuous compression or stretching of the segments. In [2] these drift velocities have been analyzed from DNS and appropriate expressions have been introduced to solve Eq. (3) numerically. The analysis has revealed that the conditional velocity difference at the ending points $\langle \Delta u|l \rangle$ is negative for small segments but scales linearly with the separation distance and is positive for larger segments, a scaling known from gradient trajectories [21,22]. Overall, the slow changes are mainly due to the continuous evolution of the bounding isosurface whose displacement in the flow field can be described by a level-set approach. The diffusion term on the r.h.s. turns out to scale as $\tilde{a}_2 \propto \tilde{a}_1 Re_\lambda^{-1/2}$ so that in the limit of large Reynolds numbers its influence on the pdf is small and can be neglected. The same is true for the term containing the time scale τ_{lm} which is the logarithmic

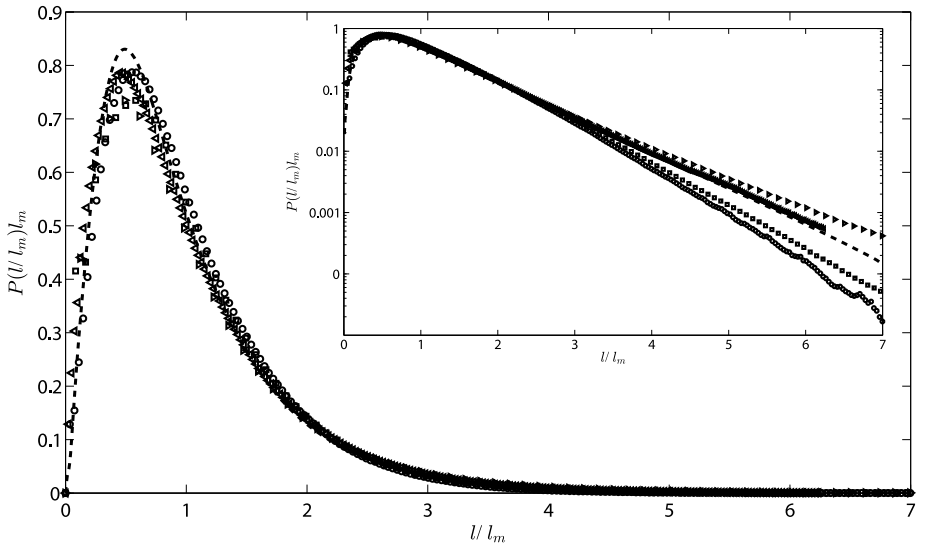

Fig. 4. Comparison of the normalized pdf $\tilde{P}(\tilde{l})$ from DNS cases 1–4 with the model solution (Eq. (3)). (○: case 1, □: case 2, ◁: case 3, ▷: case 4; - - -: model (Eq. (3)).

time rate of change of the mean length of streamline segments and is relevant for the case of decaying turbulence. However, the analysis of the DNS date revealed [2] that τ_{lm} is large so that the term can be neglected.

On the other hand, streamline segments are subject to so-called "fast changes" which are attributed to the local random distortion of the velocity field which yields non-local abrupt changes in the geometry of the streamline segment. These fast changes result in the four integral terms on the r.h.s. of Eq. (3) which have been modeled as a stationary Poisson like cutting and reconnection process with the two frequencies Λ_c (cutting frequency, corresponds to the new creation of extrema within a streamline segments and results in the cutting of the latter) and Λ_a (reconnection frequency, corresponds to the disappearance of extrema and the subsequent reconnection of two adjacent streamline segments).

It can be shown that the reconnection frequency Λ_a must be related to the diffusive drift in the origin as the latter is responsible for the disappearance of small segments due to viscous drift which directly entails the reconnection of the two adjacent segments, yielding

$$\Lambda_a \propto \left.\frac{\partial \tilde{P}}{\partial \tilde{l}}\right|_{\tilde{l}\to 0} \tag{4}$$

The remaining unknown cutting frequency Λ_c is determined during the numerical solution of Eq. (3) to ensure the normalization condition of the normalized pdf $\int_0^\infty \tilde{P}\tilde{l}\,d\tilde{l} = 1$ of the steady solution.

Based on the above modeling, the behavior of $\tilde{P}(\tilde{l})$ in the limit $\tilde{l}\to 0$ and $\tilde{l}\to\infty$ can be predicted: in the origin where Eq. (3) is dominated by the viscous drift part of the convective velocity $\tilde{a}_1$, the pdf must scale linearly while its tail for large segments will decay exponentially which is a typical feature of a Poisson process.

Fig. 4 shows the normalized pdfs $\tilde{P}(\tilde{l})$ obtained from the four DNS cases (symbols) where streamline segments are calculated from homogeneously distributed grid points in space. This procedure ensures a correct weighting of space as in general streamlines do not probe space equally resulting in a varying streamline density. In addition, homogeneously distributed grid points introduce a weighting of the pdf by a factor proportional to the length of the segments (as a twice as long segment has a twice as large probability to be counted) which as been corrected for in the post-processing of the data. Included in Fig. 4 is the steady solution of Eq. (3) where for the drift velocity the ansätze obtained in [2] have been used. A quite good agreement of the DNS data with the model can be observed, revealing the linear rise at the origin as well as the exponential tails, which are further highlighted in the log–lin inset. The maximum of all pdfs occurs at $\tilde{l}\approx 0.5$ with a value of $\tilde{P}_{max}\approx 0.75$ where the model slightly overpredicts the maxima of the DNS data which in themselves vary slightly from one DNS case to another. As the different data collapse well, the Reynolds number independence predicted by the model can be confirmed with a further independence of the type of the flow under consideration as the data not only contain homogeneous isotropic decaying cases, but also a forced and a homogeneous shear flow. In addition, the model shows that the only relevant length scale of the distribution of the length of streamline segments is the mean length l_m. This raises the question how the mean length scales with turbulent length scales of the flow under consideration, a question that will be addressed in the following section.

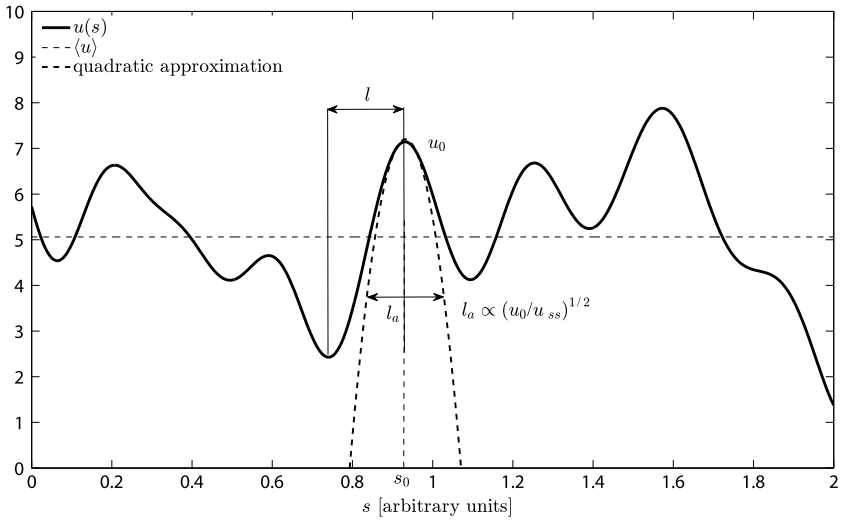

Fig. 5. Local expansion of the u profile in an extremum along the streamline coordinate s.

5. Scaling of the mean length

Introduction of the unit tangent vector t_i into Eq. (1) yields after integration a space curve parameterized with its own arclength s which can be obtained by integration of $\mathrm{d}s = u\,\mathrm{d}\hat{\tau}$. Then along a streamline the arclength s serves as a one-dimensional coordinate and the variation of the absolute value $u(s)$ can be viewed as a one-dimensional variation along s.

Let us in this context determine the life-time of an extreme point. The vicinity of an extreme point is mainly diffusion controlled so that in a coordinate system moving with it (Lagrangian view) we can model the evolution of the u profile by a simple diffusion equation

$$\frac{Du}{Dt} \approx \nu \frac{\partial^2 u}{\partial s^2} \tag{5}$$

Within this framework we can estimate its characteristic life-time t_a as

$$t_a \propto \frac{l_a^2}{\nu} \tag{6}$$

where l_a denotes its characteristic size. Note that the inverse of the time scale t_a must be proportional to the reconnection frequency μ_a (which corresponds to the non-dimensional frequency Λ_a in the model pdf Eq. (3)) yielding

$$t_a^{-1} \propto \mu_a \tag{7}$$

as the disappearance of an extreme point along the streamline yields the reconnection of the two adjacent segments. The size of the extreme point l_a can be estimated as follows by an expansion of the scalar field u around it yielding

$$u = u_0 + \frac{1}{2}u_{ss}(s-s_0)^2 + \mathcal{O}\big(s^3\big) \approx u_0\left[1 + \frac{u_{ss}}{2u_0}(s-s_0)^2\right] \approx u_0\left[1 + \left(\frac{(s-s_0)}{l_a}\right)^2\right] \tag{8}$$

where u_0 is the value of the scalar at the extreme point and $u_{ss} = \partial^2 u/\partial s^2$ is its second derivative in direction of the streamline evaluated at the extreme point which is located at s_0. Fig. 5 illustrates the scenario along a streamline and displays all relevant scales. In particular, it becomes obvious that the size of the extremum l_a is proportional to the size of the segment l under consideration.

From the last identity we see that the instantaneous characteristic size of an extreme point can be estimated as

$$l_a^2 \propto \frac{u_0}{u_{ss}} \tag{9}$$

Assuming statistical independence of u_0 and u_{xx} at the extreme point let us average over all extrema to obtain

$$\langle l_a \rangle \propto \left(\frac{\langle u^2 \rangle^{1/2}}{\langle u_{ss}^2 \rangle^{1/2}}\right)^{1/2} \tag{10}$$

Note the similarity to the result obtained by Rice's theorem [23,24] for the zero crossings of u, i.e. the mean distance of stagnation points. However, in our case the second derivative comes into play as we are considering the zero crossings of the gradient of u rather than of u itself.

Table 2
Statistical parameters of the streamline segment analysis.

DNS case	1	2	3	4
Flow type	Decaying	Decaying	Forced	Shear
Reynolds number Re_λ	50	116	206	300
Mean length l_m	0.109	0.047	0.078	0.058
Ratio l_m/λ	0.780	0.618	0.534	0.552
Ratio l_m/η	10.90	13.10	15.00	18.70
Ratio $l_m/(\lambda\eta)^{1/2}$	2.924	2.841	2.831	3.215

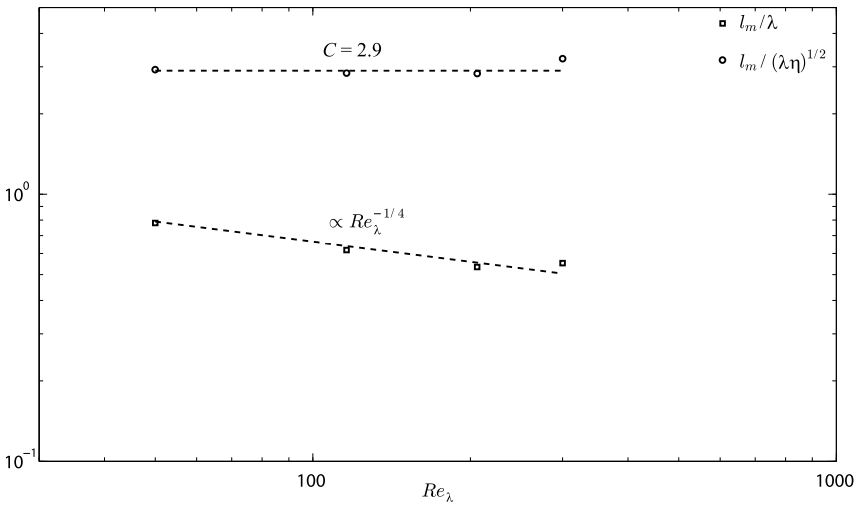

Fig. 6. Scaling of the mean length of streamline segments with the Taylor microscale and the new scaling (Eq. (14)) over the Taylor based Reynolds number from DNS cases 1–4.

Following Kolmogorov's similarity hypothesis [3,25], the root-mean-square (rms) of the second derivative u_{ss}, being a purely small scale quantity, should scale solely with the mean energy dissipation ε and the viscosity ν yielding

$$\langle u_{ss}^2 \rangle^{1/2} \propto \varepsilon^{3/4} \nu^{-5/4} \tag{11}$$

With Eq. (11) we obtain the following scaling of the mean size of extrema of u along streamlines

$$\langle l_a \rangle \propto \left(u_{rms} \varepsilon^{-3/4} \nu^{5/4} \right)^{1/2} \propto \lambda \, Re_\lambda^{-1/4} \propto (\lambda\eta)^{1/2} \tag{12}$$

with the Kolmogorov scale $\eta = (\nu^3/\varepsilon)^{1/4}$ and the Taylor microscale $\lambda = (15\nu u_{rms}^2/\varepsilon)^{1/2}$.

At this point we only have to show that indeed the mean size of the extrema scales with the mean length of the streamline segments (with a numerical constant that is independent of the Reynolds number). To this end let us use Eq. (7) in combination with Eq. (4) to obtain

$$t_a^{-1} \propto \mu_a \propto \nu \left. \frac{\partial P}{\partial l} \right|_{l \to 0} \propto \frac{\nu}{l_m^2} \left. \frac{\partial \tilde{P}}{\partial \tilde{l}} \right|_{\tilde{l} \to 0} \propto \frac{\nu}{l_m^2} \tag{13}$$

where the slope in the origin of the compensated pdf $\partial \tilde{P}/\partial \tilde{l}$ is a universal, Reynolds number independent constant (or in other words, the non-dimensional frequency Λ_a is Reynolds number independent). Comparison of Eq. (13) with Eq. (6) yields finally

$$\langle l_a \rangle \propto l_m \propto \lambda \, Re_\lambda^{-1/4} \propto (\lambda\eta)^{1/2} \tag{14}$$

Introduction of Eq. (14) into (13) yields for the reconnection time t_a

$$t_a \propto u_{rms} \varepsilon^{-3/4} \nu^{1/4} \tag{15}$$

which corresponds to the Tennekes Lagrangian time t_l, cf. [26].

Table 2 shows that the above scaling of the mean length of streamline segments is valid for all four cases under consideration and thus seems to hold over a broad range of Reynolds numbers. While the ratio of l_m with neither the Kolmogorov length scale nor the Taylor microscale yields a Reynolds number independent constant, the value of the constant for a normalization following the scaling of Eq. (14) yields a constant $C \approx 2.9$ for all three cases where only the shear case, probably

due to the anisotropic influence of the constant shear gradient, yields a slightly larger value than the three other cases. This finding is further highlighted in Fig. 6 where the ratio l_m/λ and the ratio $l_m/(\lambda\eta)^{1/2}$ are shown over the Taylor based Reynolds number in a double logarithmic plot, indicating a clear scaling with $Re_\lambda^{-1/4}$ of the former and a Reynolds number independent constant of the latter.

6. Conclusion

The analysis of turbulent flow fields via streamline segments has been extended to the DNS of flow fields other than homogeneous isotropic decaying turbulent fields which now cover a range of Reynolds numbers from $Re_\lambda = 50$–300. Special attention was given to the normalized pdf of the length of streamline segments, which turns out to be Reynolds number independent when normalized with the mean length l_m. A model for the pdf which has been derived in [2] is reviewed and was found to also be in good agreement with the new DNS cases confirming the assertion that in the context of streamline segments there exists only one relevant length scale, namely the mean length l_m. In addition, the main features of the surface containing all ending points of streamline segments have been reviewed, namely the fact that in this surface all local extrema of the turbulent kinetic energy field are contained. These points also include stagnation points of the flow field as these are minima of the turbulent kinetic energy. In a second step, a new scaling law of the mean length of streamline segments in turbulent flows has been derived based on theoretical considerations on the size of local extrema of the absolute value of the velocity field u along the streamline which demark the ending points of streamline segments. A scaling argument based on Kolmogorov's similarity hypotheses yields that, in close connection to the well known Rice theorem, the mean distance between two extrema along a streamline should scale with geometrical mean of the Kolmogorov scale η and the Taylor microscale λ so that $l_m \propto (\eta\lambda)^{1/2}$. This scaling could be confirmed for all four DNS cases under consideration and the proportionality constant turns out to be close to a numerical value of 2.9.

Acknowledgements

This work was funded by the Deutsche Forschungsgemeinschaft under Grant Pe 241/38-2 and supported by the Gauss Center for Supercomputing. The author would like to thank J.H. Goebbert for his continuous support concerning numerical procedures and in particular his support regarding the visualizations.

References

[1] L. Wang, On properties of fluid turbulence along streamlines, J. Fluid Mech. 648 (2010) 183–203.
[2] P. Schaefer, M. Gampert, N. Peters, The length distribution of streamline segments in homogeneous isotropic decaying turbulence, Phys. Fluids 24 (2012) 045104.
[3] A.N. Kolmogorov, The local structure of turbulence in an incompressible viscous fluid for very large Reynolds numbers, Dokl. Akad. Nauk SSSR 30 (1941) 301–305.
[4] U. Frisch, Turbulence: The Legacy of A.N. Kolmogorov, Cambridge University Press, 1995.
[5] S. Corrsin, Random geometric problems suggested by turbulence, in: M. Rosenblatt, C. van Atta (Eds.), Statistical Models and Turbulence, in: Lecture Notes in Physics, vol. 12, Springer Verlag, 1971, pp. 300–316.
[6] Z.S. She, E. Jackson, S.A. Orszag, Intermittent vortex structures in homogeneous isotropic turbulence, Nature 344 (1990) 226–228.
[7] Y. Kaneda, T. Ishihara, High-resolution direct numerical simulation of turbulence, J. Turbulence 7 (2006) 1–17.
[8] L. Wang, N. Peters, The length scale distribution function of the distance between extremal points in passive scalar turbulence, J. Fluid Mech. 554 (2006) 457–475.
[9] L. Wang, N. Peters, Length scale distribution functions and conditional means for various fields in turbulence, J. Fluid Mech. 608 (2008) 113–138.
[10] C.H. Gibson, Fine structure of scalar fields mixed by turbulence. I. Zero gradient points and minimal gradient surfaces, Phys. Fluids 11 (1968) 2305–2315.
[11] P. Schaefer, M. Gampert, J.H. Goebbert, L. Wang, N. Peters, Testing of different model equations for the mean dissipation using Kolmogorov flows, Flow Turbul. Combust. 85 (2010) 225–243.
[12] P. Rao, Geometry of streamlines in fluid flow theory, Def. Sci. J. 28 (1978) 175–178.
[13] W. Braun, F.D. Lillo, B. Eckhardt, Geometry of particle paths in turbulent flows, J. Turbul. 7 (2006) 1–10.
[14] A. Scagliarini, Geometric properties of particle trajectories in turbulent flows, J. Turbul. 12 (2011).
[15] P. Schaefer, Curvature statistics of streamlines in various turbulent flows, J. Turbul. 13 (1) (2012) 28.
[16] S. Goto, D.R. Osborne, J.C. Vassilicos, J.D. Haigh, Acceleration statistics as measures of statistical persistence of streamlines in isotropic turbulence, Phys. Rev. E 71 (2005).
[17] S. Goto, J.C. Vassilicos, Particle pair diffusion and persistent streamline topology in two-dimensional turbulence, New J. Phys. 6 (2004) 65.
[18] J. Soria, B. Cantwell, Topological visualisation of focal structures in free shear flows, Appl. Sci. Res. 53 (1994) 375–386.
[19] P. Schaefer, M. Gampert, J. Goebbert, M. Gauding, N. Peters, Asymptotic analysis of homogeneous isotropic decaying turbulence with unknown initial conditions, J. Turbul. 12 (2011) 1–20.
[20] M. Gampert, J.H. Goebbert, P. Schaefer, M. Gauding, N. Peters, F. Aldudak, M. Oberlack, Extensive strain along gradient trajectories in the turbulent kinetic energy field, New J. Phys. 13 (2011) 043012.
[21] P. Schaefer, M. Gampert, N. Peters, Joint statistics and conditional mean strain rates of streamline segments, Phys. Scr. T (2012), in press.
[22] M. Gampert, P. Schaefer, J. Goebbert, N. Peters, Decomposition of the field of the turbulent kinetic energy into regions of compressive and extensive strain, Phys. Scr. T (2012), in press.
[23] S. Rice, Mathematical analysis of random noise, Bell Syst. Tech. J. 23 (282) (1944).
[24] S. Rice, Mathematical analysis of random noise, Bell Syst. Tech. J. 24 (46) (1945).
[25] A.N. Kolmogorov, Dissipation of energy under locally isotropic turbulence, Dokl. Akad. Nauk SSSR 32 (1941) 16–18.
[26] H. Tennekes, Eulerian and Lagrangian time microscales in isotropic turbulence, J. Fluid Mech. 67 (1975) 561–567.